








Nature-based solutions in mountain catchments reduce impact of anthropogenic climate change on drought streamflow

Petra B. Holden ^{1✉}, Alanna J. Rebelo ², Piotr Wolski ³, Romaric C. Odoulami ¹, Kamoru A. Lawal ¹, Joyce Kimutai^{1,4}, Tiro Nkemelang ¹ & Mark G. New ^{1,5}

Quantifying how well Nature-based Solutions can offset anthropogenic climate change impacts is important for adaptation planning, but has rarely been done. Here we show that a widely-applied Nature-based Solution in South Africa – invasive alien tree clearing – reduces the impact of anthropogenic climate change on drought streamflow. Using a multi-model joint-attribution of climate and landscape-vegetation states during the 2015–2017 Cape Town “Day Zero” drought, we find that anthropogenic climate change reduced streamflow by 12–29% relative to a counterfactual world with anthropogenic emissions removed. This impact on streamflow was larger than corresponding reductions in rainfall (7–15%) and reference evapotranspiration (1.7–2%). Clearing invasive alien trees could have ameliorated streamflow reductions by 3–16% points for moderate invasions levels. Preventing further invasive alien tree spread avoided potential additional reductions of 10–27% points. Total clearing could not have offset the anthropogenic climate change impact completely. Invasive alien tree clearing is an important form of catchment restoration for managing changing hydroclimatic risk, but will need to be combined with other adaptation options as climate change accelerates.

¹African Climate and Development Initiative, University of Cape Town, Cape Town, South Africa. ²Department of Conservation Ecology and Entomology, Stellenbosch University, Stellenbosch, South Africa. ³Climate System Analysis Group, University of Cape Town, Cape Town, South Africa. ⁴Kenya Meteorological Department, Nairobi, Kenya. ⁵Department of Environmental and Geographical Science, University of Cape Town, Cape Town, South Africa. ✉email: petra.holden@uct.ac.za

Earth's climate is changing due to anthropogenic emissions of greenhouse gases (GHG), and with it extreme weather events, such as droughts and floods^{1,2}. Impacts of extreme events on people arise from the climate phenomena but also the sensitivity of the receiving biophysical environment. One can assume a causal chain of links between drivers, pressures, states, impacts and responses related to extreme events. Drivers (such as trends in economic sectors and industry) exert pressures (such as GHG emissions) on the state of the physical climate which then impacts on people. As emission reduction strategies targeted at the main driving forces and pressures have, to date, been limited, there has been a focus on implementing local scale climate change adaptation actions that reduce the sensitivity of the biophysical receiving environment³. For example, ecosystem management, protection and restoration have been proposed for buffering societies from the increased impact of climate-related extremes due to anthropogenic climate change (ACC)^{4–6}.

These interventions, termed Nature-based Solutions (NbS) for climate change adaptation, are framed as being able to reduce or even offset the impacts experienced from anthropogenic influence on the physical climate system and in particular those impacts related to changing extreme events. Examples include restoring or protecting riverbanks, wetlands and catchment headwaters to reduce erodibility, ensure water security through increasing water yields, and protect communities from flooding from rainfall extremes^{7,8}. Despite the popularity of NbS in policy and research, and the growing literature on the use of NbS as an adaptation response, there is very little quantitative evidence of their effect in modulating the biophysical impacts that result from anthropogenic influence on extreme weather and climate events^{9–12}.

Quantitative assessments of the impact of NbS often focus on climate change mitigation potential including how much carbon they can remove from the atmosphere^{13–15}, or more recently NbS effects on global temperatures¹⁶. These analyses are mostly global despite the scale at which the impacts of ACC on extremes are felt and at which climate adaptation decisions are made. This makes it difficult for results to directly inform regional and local level decision-making processes². Thorough reviews do exist that summarise the extensive evidence base on the role of NbS for climate change adaptation^{7,9,10} or ecosystems in reducing disaster risk¹⁷. While the studies included and synthesised in these reviews have been conducted at a useful scale for decision making, they focus on climate-related impacts and thus do not isolate the impact of NbS on the ACC-derived portion of the impact experienced, especially for extreme events that have already occurred. For example, few studies have attributed biophysical impacts to ACC influence on the actual extreme event (i.e., changes to the extreme event due to ACC) while simultaneously evaluating the role of the NbS in modulating this impact. Furthermore, existing reviews that have focused on the potential of ecosystems for reducing disaster risk or NbS as a climate change adaptation option have shown that there is insufficient relevant research that considers locally and nationally relevant NbS options in the Global South^{10,17}.

Quantifying the potential of NbS for managing the impact of extreme events due to ACC is challenging. This is due to a lack of sampling distribution, as we only experience one extreme event and one type of landscape state, i.e., in a world with GHG emissions and with observed levels of human influence on the landscape, and no counterfactual, i.e., a world with no human influence on atmospheric conditions and landscapes. Also, no single extreme event can be attributed to ACC alone. Every extreme weather event is unique and always the result of a combination of both human-induced and natural drivers of climate change, as well as internal climate variability. This makes it impossible to say that an event could not have occurred without

anthropogenic influence. However, the presence of ACC can alter the characteristics of extreme weather events¹⁸. We need methods to be able to quantify the role of ACC in changing extreme event characteristics from a meteorological perspective that can also be used to quantify the role that NbS play in moderating this impact. The science of extreme weather and climate event attribution provides a promising framework to achieve this. Over the last few years, substantial advances have been made in this field².

There are now numerous examples of extreme weather and climate event attribution studies, which have quantified the extent to which ACC altered the characteristics of a specific observed extreme event^{19,20}. The framework of event attribution has been developed and applied primarily for meteorological events²¹. For example, attribution studies have focused on physical climate variables associated with specific extremes such as rainfall, temperature, or relevant indices that use these variables. A few studies have gone further to assess the propagation of human influence on climate extremes through to an attributable impact on hydrological systems or society: examples include flooding in the United Kingdom^{22–24} and Okavango, Botswana²⁵, streamflow in the USA²⁶ and human mortality associated with heat waves in Paris and London²⁷.

We draw on the methods of event attribution science and apply them to attribute the potential for NbS to moderate the impact of ACC on the Cape Town Day Zero drought (2015–2017), a very rare event and the worst in the region since 1904^{28,29}. Cape Town's water supply is dependent on streamflow from a relatively small area made up of several mountainous headwater catchments. The streamflow from these catchments is captured and stored in six large dams^{30,31}. During the drought, dam levels dropped to <20% of their capacity which forced Cape Town to prepare for the day when the taps would run dry (Day Zero)³². Evidence shows that ACC increased the likelihood of the rainfall deficit in the broader southwestern Cape region by a factor of three³¹ to six³². Here we adopt a high-resolution hydrological modelling perspective to zoom into these critical water source areas for Cape Town, to determine: (i) whether ACC-reduced streamflow in these areas during the drought relative to a world without ACC, and if it did; (ii) whether NbS through complete restoration of these water source areas before the drought hit in 2015 could have reduced or offset this impact; and (iii) whether the limited restoration that had occurred prior to the drought played any role in avoiding potential escalated impact of ACC.

In terms of NbS, we focus on a widely implemented and relevant form of restoration in South Africa: invasive alien tree (IAT) clearing. IATs are a major threat to water security especially in the Western Cape of South Africa and for Cape Town's water supply. They have spread along riparian zones and upslope into mountains and have been shown, through paired-catchment and modelling studies, to use substantially more water in comparison to the native shrublands³³. The natural vegetation of the region, known as fynbos, is comprised of evergreen shrubs and graminoids (grass-like plants), with no tree element except in ravines. Many parts of these critical water source areas are relatively undeveloped or untransformed, apart from the areas that are invaded by IATs, mainly *Acacia mearnsii*; *Pinus* spp., *Eucalyptus* spp. and *Acacia longifolia*. IATs alter vegetation water-use characteristics in ways that reduce runoff and decrease groundwater recharge. For example, the trees are taller, and have greater leaf area indices and deeper root systems, compared to the native vegetation of the region and therefore have higher transpiration rates and thus reduce streamflow including baseflow. For paired-catchment studies in winter-dominated rainfall areas in South Africa, the impact of IAT and afforestation has been shown to be experienced mostly during dry periods, droughts and dry seasons, when water is most needed³⁴.

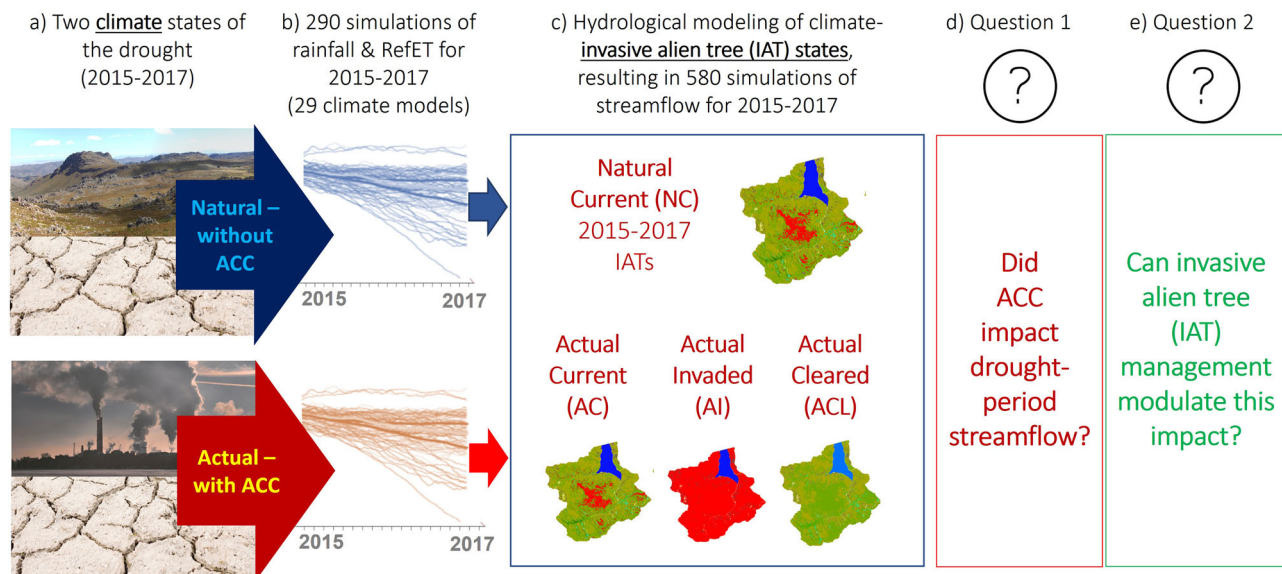


Fig. 1 Modelling set-up for joint multi-model event attribution (Climate and IAT states) applied in this paper. The joint multi-model event attribution framework, showing one catchment as an example: the Upper Berg, South Africa. **a, b** Illustrates the simulations of climate variables for the Cape Town ‘Day Zero’ Drought under today’s climate (Actual) and a counterfactual climate (Natural) with human-induced drivers removed, **c** shows the three different invasive alien tree (IAT) states resulting in hydrological modelling of four climate-IAT states: Natural Current (NC), Actual Current (AC), Actual Invaded (AI), Actual Cleared (ACL). This enabled us to determine the percentage of Natural Climate drought-period streamflow realised under the Actual Climate with the observed levels of IATs (as described in ref. 67) that were present during the drought (Current Landscape); and the extent to which management of IATs could have modulated any reductions or changes in drought-period streamflow due to anthropogenic climate change (**d, e**).

This phenomenon is not unique to South Africa. There have been similar results reported in other water-limited environments and/or winter rainfall-dominated areas through both modelling and paired-catchment studies^{35–39}. For example, in trading water for carbon, it has been repeatedly shown that replacing native grasslands with afforestation reduces streamflow⁴⁰. Furthermore, reviews of paired-catchment studies and modelling of watersheds across the globe have shown decreases in streamflow due to afforestation in ecosystems with previously shorter vegetation, such as grasslands or shrublands^{35,39}. For example, out of 308 individual studies across the globe (including Oceania, Europe, Asia and the Middle East, North America, Central and South America and Africa) 80% reported a decrease in water yield in response to afforestation actions. When isolating the baseflow components of the yields, 63% showed a decrease in baseflows due to afforestation actions (i.e., non-native tree species)⁴¹. This impact on baseflows might be surprising but even when afforestation or tree invasion increases infiltration relative to the natural conditions, low flow can still decrease because more soil water is transpired, leaving little for aquifer recharge³⁶. Despite global concerns and restoration efforts at local and regional scales, IATs continue to proliferate in many areas, resulting in multiple challenges for countries across the globe^{42,43}, but especially in water-stressed environments^{34,44,45}. Woody tree and plant encroachment in grasslands and savannas has also increased worldwide, especially in the rangelands of America, Australia and southern Africa⁴⁶.

To quantify the impact of ACC and IAT clearing or lack thereof on drought-period mean streamflow, we applied a joint event attribution framework (Fig. 1) to two headwater catchments, the Upper Berg (78 km²) and Du Toits (46 km²), which supply water impoundments of critical importance to the metropolitan area of Cape Town, the surrounding rural communities and irrigated agriculture in the region (Fig. 2 and Methods).

We extend previous multi-model climate attribution approaches^{18,19} by using linked climate and hydrological model simulations

(Fig. 1 and Table 1) to attribute the relative contributions of ACC and level of IAT cover to drought-period streamflow. This comprised simulating daily streamflow for the drought period, 2015–2017, using climate change attribution inputs for daily rainfall and reference evapotranspiration from three climate model experiments (Fig. 1, Table 1, Methods and Supplementary Fig. 1). We did this based on four climate-IAT states including a reference state (Natural Current [NC]) comprised of a Natural climate with anthropogenic emissions removed with Current levels of IATs (the actual invasion present during the drought period), and three comparator states for an Actual climate with anthropogenic emissions: (i) Actual climate with Current IAT (Actual Current [AC]); (ii) Actual climate with completely cleared IAT (Actual Cleared [ACL]); and (iii) Actual climate with full catchment IAT cover (Actual Invaded [AI]) (Fig. 3). Comparing each of these three states to the reference allowed us to quantify the relative contribution of climate change and IAT on drought-period streamflow, including (i) the attributable ACC influence on drought-period streamflow through changes in rainfall and evaporation; (ii) the extent to which clearing the catchments could have offset this ACC impact; and (iii) the extent to which full catchment IAT invasion could have exacerbated the ACC impact.

Climate change attribution inputs for the hydrological model were derived from a 68-member ensemble from the Hadley Centre Regional Model (HadRM3P) nested in the Hadley Centre Global Atmospheric Model (HadAM3P-N96) from the weather@home modelling system (referred to as W@home); a 50-member ensemble from one model (ECHAM5.4) contributing to the Climate of the 20th Century Plus (C20C+) Detection and Attribution project (referred to as C20C); and a 27-member multi-model ensemble from the fifth phase of the Coupled Model Intercomparison Project (referred to as CMIP5) (Methods). We used these climate change attribution simulations as inputs to a locally validated, physically based hydrological model (MIKE SHE) coupled with a channel routing model (MIKE HYDRO)

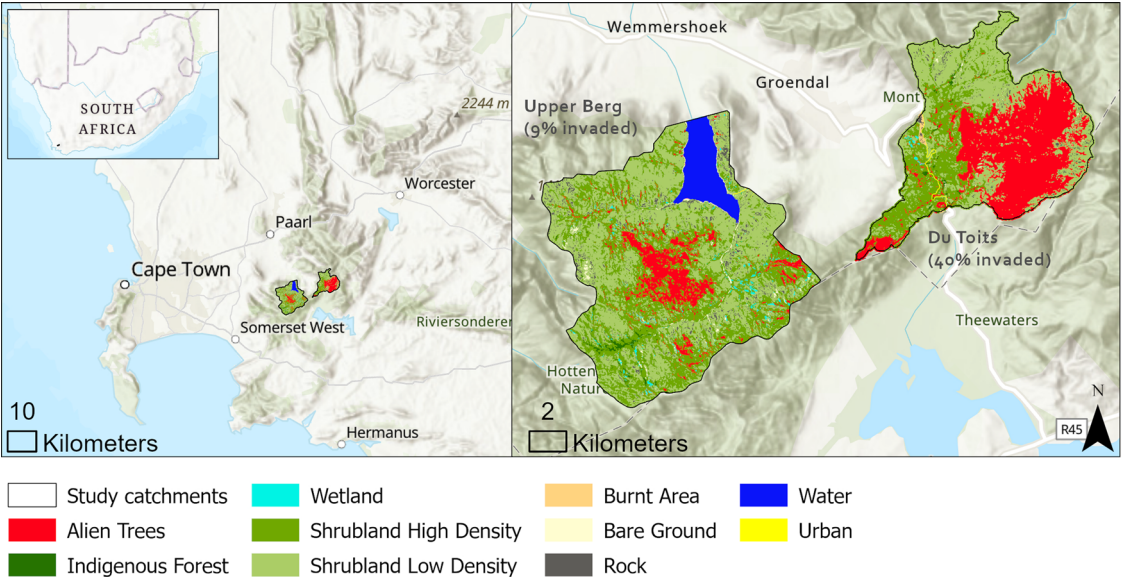


Fig. 2 Study catchments. Mountainous catchments, the Upper Berg and Du Toits, critical for water supply to the City of Cape Town in South Africa, and the level of invasive alien tree (IAT) infestations during the drought period (as described in ref. 67). Base map: Esri, NASA, NGA, USGS, Esri South Africa, HERE, Garmin, METI/NASA, FAO, NOAA.

Table 1 A description of the climate-invasive alien tree states (climate-IAT states) for the Cape Town Drought, South Africa.		
Climate-IAT states	Abbrev.	Description
Natural + Current	NC	Natural (N) climate state with <u>C</u> urrent (C) (2019) levels of IATs (9% - Upper Berg; 40% Du Toits)
Actual + Current	AC	<u>A</u> ctual (A) climate state with <u>C</u> urrent (C) (2019) levels of IATs (9% Upper Berg; 40% Du Toits)
Actual + Invaded	AI	<u>A</u> ctual (A) climate state with catchments fully <u>I</u> nvaded (I) with IATs in areas available for invasion (90% Upper Berg; 98% Du Toits)
Actual + Cleared	ACL	<u>A</u> ctual (A) climate state with catchments fully <u>C</u> leared (CL) of IATs from the current state

For the climate states, the Actual conditions represented the climate for the drought as we experienced it whereas the Natural conditions represented the drought as it might have been without human influence on atmospheric composition. For the landscape states, the Current conditions represented the landscape for the drought as we experienced it, whereas the Invaded and Cleared conditions represented the drought as it might have been with clearing observed levels of IATs and without maintenance and allowing spread to full catchment, respectively (Fig. 3).

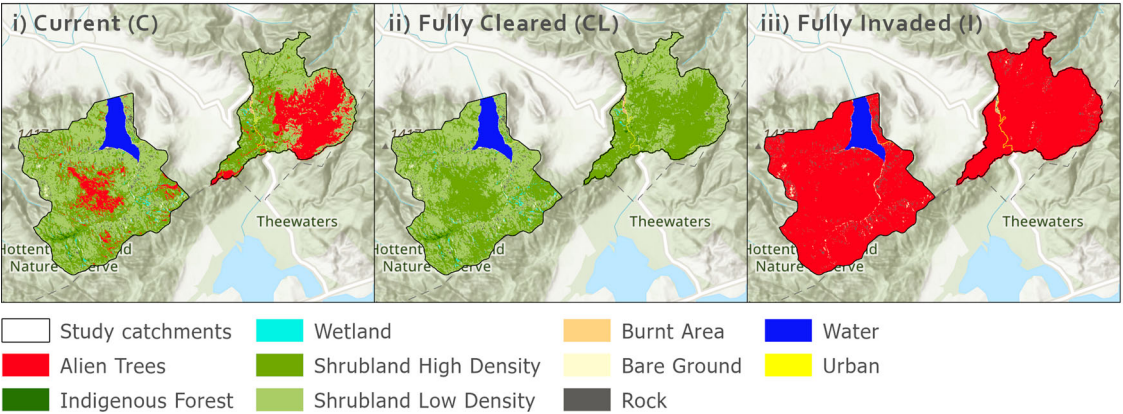


Fig. 3 Invasive alien tree (IAT) states. The three IAT landscape states used in the hydrological modelling (i) Current (C) state which reflects invasion levels present during the drought (2015–2017); (ii) Fully Cleared (CL) state representing all IATs cleared; and (iii) fully Invaded (I) state representing lack of maintenance of cleared areas and spread to full catchment invasion. Base map: Esri, NASA, NGA, USGS, Esri South Africa, Esri, HERE, Garmin, FAO, METI/NASA, USGS.

(Methods). Thus, each climate-IAT state was represented by an ensemble of 145 hydrological model simulations (alternative realisations) of the climate and IAT state during the 2015–2017 drought period.

We used two main metrics to quantify the impact of ACC on drought-period streamflow and the difference that invasion or

clearing could have had on this impact: (i) QR%, which is the percentage of reference state (Natural Current) drought-period streamflow realised for each comparator state (Actual Current, -Cleared, -Invaded); and (ii) QR% point difference, which is the percentage point difference between the QR% derived for the Actual Current state and that derived for the two other

comparator states (Actual Cleared, -Invaded). For ease, we also show and refer to the percentage change in drought-period streamflow relative to the reference state (% Change in QR) which is the inverse of QR% (i.e., if QR% is 85% the % Change in QR is -15%). To provide an indication of confidence in the estimates derived for each of these metrics (QR%, % Change in QR, QR% point difference) we use a bootstrap percentile confidence interval methodology^{47,48} which is applied to the mean drought-period streamflow simulated for each climate model experiment separately. We analyse the results of the resampled drought-period streamflow separately for each climate model experiment but also synthesise these across the climate model experiments (Methods and Supplementary Methods 1).

Based on the analysis of factual and counterfactual simulated streamflow for the Cape Town Day Zero drought, we provide quantitative evidence that NbS can be an effective adaptation approach to support drought impact reduction in a changing climate. We find that IAT management, including IAT clearing and preventing IAT spread, has the potential to ameliorate, but not eliminate, attributable ACC impacts on drought streamflow. The results are relevant to water-limited environments that are experiencing woody encroachment due to IATs and/or woody indigenous vegetation^{37,41,46,49–51}. Our findings however point to the need for NbS to be fully integrated into wider adaptation portfolios. This is because despite showing that IAT management is important for reducing ACC impact on drought streamflow, we also show that it could not completely offset the anthropogenic component of the drought we studied.

Results

ACC impact on drought-period streamflow. We first assess the change in drought-period streamflow attributable to ACC for the observed levels of IATs that were present in each catchment during the 2015–2017 period. The multi-model synthesis drought-period mean streamflow ratio (QR), expressed as a percentage (QR%) is 83 (95%CI: 78–88) and 78 (95%CI: 71–85) for the Berg and Du Toits, respectively (Fig. 4). Therefore, simulated results showed that ACC altered drought-period streamflow relative to a world without anthropogenic climate by -17% (95%CI: -22 , -12%) and -22% (95%CI: -29 , -15%) in the Berg and Du Toits, respectively (Fig. 4 and Supplementary Table 1). When considered individually, each model experiment (C20C, CMIP5, and W@home) also showed an attributable decrease in drought-period streamflow relative to a natural climate, due to ACC at the 95% confidence level (Fig. 4 and Supplementary Table 1).

The role of IAT management in reducing ACC impact. We next assess the role of IAT management in modulating the impact of ACC on drought-period streamflow. Simulations showed that clearing IATs prior to the drought would have likely ameliorated the reductions in drought-period streamflow experienced due to ACC, but that this depended on the extent of invasion (Figs. 4–5 and Supplementary Table 2). For example, simulations showed that clearing the 40% invaded area in the Du Toits catchment before the drought hit in 2015 would have offset the streamflow impact somewhat, shifting it from 78% (95%CI: 71, 85) to 87% (95%CI: 80, 94) (Fig. 4 and Supplementary Table 1). Thus, clearing would have resulted in a 9%-point gain (95%CI: $+3$, $+15\%$ points) in drought-period streamflow in a world with ACC, a clearly attributable effect of NbS at the 95% confidence interval (Fig. 5 and Supplementary Table 2). In contrast, for the Upper Berg, the results show that we cannot detect—at the 95% confidence level—an attributable impact on drought-period streamflow of clearing the much smaller extent of aliens (9% invasion) that were present. Here

the change in streamflow from clearing was $+1\%$ (CI: -4% , $+6\%$) (Fig. 5 and Supplementary Table 2).

Extensive clearing, however, had already been implemented in the Upper Berg prior to the drought to reduce the invasions down to the current 9% levels. This mostly took place between 2006 and 2010 when the former state forestry plantation areas were cleared, followed by natural regeneration of the vegetation, but maintenance and follow-up clearing have continued from 2010 under South Africa's Working for Water programme⁵². It is therefore likely that if this clearing had not been implemented and maintained, the impacts of ACC on the water shortages in the Berg water impoundment would have been further exacerbated. For example, if the invasion had not been managed, and the catchments had become fully invaded at the time of drought, the impact of ACC on drought-period streamflow would have been aggravated (Figs. 4–5 and Supplementary Tables 1–2). The multi-model drought-period streamflow ratio, expressed as a percentage (QR %) for the Actual Climate with fully invaded catchments (AI: Actual Invaded) is 69% (95%CI: 64, 74) and 57% (95%CI: 52, 63) for the Upper Berg and Du Toits respectively. This equates to a change in drought-period streamflow in comparison to a Natural Climate with observed levels of IATs (Natural Current) of -31% (95%CI: -36 , -26) and -43% (95%CI: -48 , -37) (Fig. 4 and Supplementary Table 1). Thus, in comparison to the drought as was experienced with ACC and with the observed levels of IATs, allowing the spread of IATs to the entire catchment would have further escalated reductions of Natural Climate streamflow realised with ACC by -14 (95%CI: -19 , -10) and -21 (95%CI: -27 , -14) % points (Fig. 5 and Supplementary Table 2). Therefore, if the observed levels of IATs were not maintained in the catchments and IATs had spread to cover the full catchments, it is likely that the water shortages experienced by the city of Cape Town would have been exacerbated due to the further reductions in streamflow realised in these catchments.

Despite the positive impact of clearing and preventing the spread of IATs on ameliorating or preventing escalation in the reductions of drought-period streamflow experienced due to ACC, in all cases clearing the observed levels of IATs was not able to remove the full ACC signal. Even with the full clearing of both catchments there remained an effect of ACC on drought-period streamflow i.e., the 95% confidence intervals shown in Fig. 4 do not shift to contain 100% even when all the IATs are cleared in the catchments. For example, the QR% for each catchment is 84 (95%CI: 79, 90) and 87 (95%CI: 80, 94) even when cleared. This means that even with completely cleared catchments we would not have realised 100% or more of the Natural Climate streamflow due to ACC.

The relative role of the impact of ACC on reference evapotranspiration versus rainfall on streamflow. We next focus on how the impact of ACC differed between the driving climate variables (rainfall and reference evapotranspiration) and the resulting drought-period streamflow. ACC reduced drought-period rainfall to between 85% and 93% (95%CI across both catchments) of that under a Natural Climate (Supplementary Notes 1, Supplementary Figs. 2–3 and Supplementary Table 3). This reduction is less than that for streamflow (95%CI: 71–88% across both catchments, Fig. 4, and Supplementary Table 1). This shows that catchment hydrological processes exacerbated the ACC signal as it propagated from drought-period rainfall through the catchment hydrological system to streamflow. We also find a small but attributable ACC impact on reference evapotranspiration. The multi-model synthesis drought-period mean reference evapotranspiration ratio (expressed as a percentage) is 101.84% (95%CI: 101.69, 101.99), and all individual experiments also show

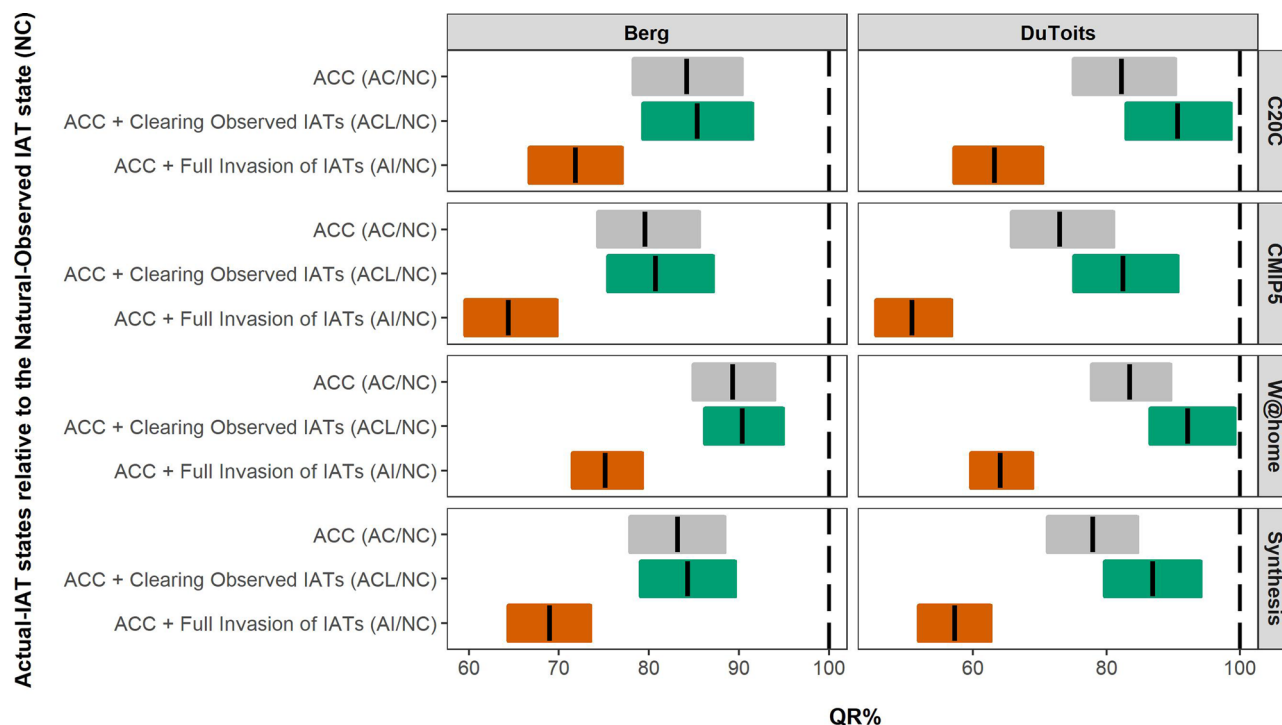


Fig. 4 The percentage of drought-period streamflow (QR%) under natural climate realised during the drought period attributable to anthropogenic climate change (ACC) combined with different IAT states. For each catchment (Berg and Du Toits, South Africa), the percentage reference state (Natural Current) drought-period streamflow is shown for each comparator state (Actual Current, -Cleared, -Invaded) (also see Supplementary Table 1). Changes are shown for each climate model experiment (C20C, CMIP5 and W@home) and for the multi-model experiment synthesis (Synthesis). The solid line is the median change, while the coloured bar shows the 95% confidence interval (Methods and Supplementary Methods 1). NC Natural Current, AC Actual Current, ACL Actual Cleared, AI Actual Invaded.

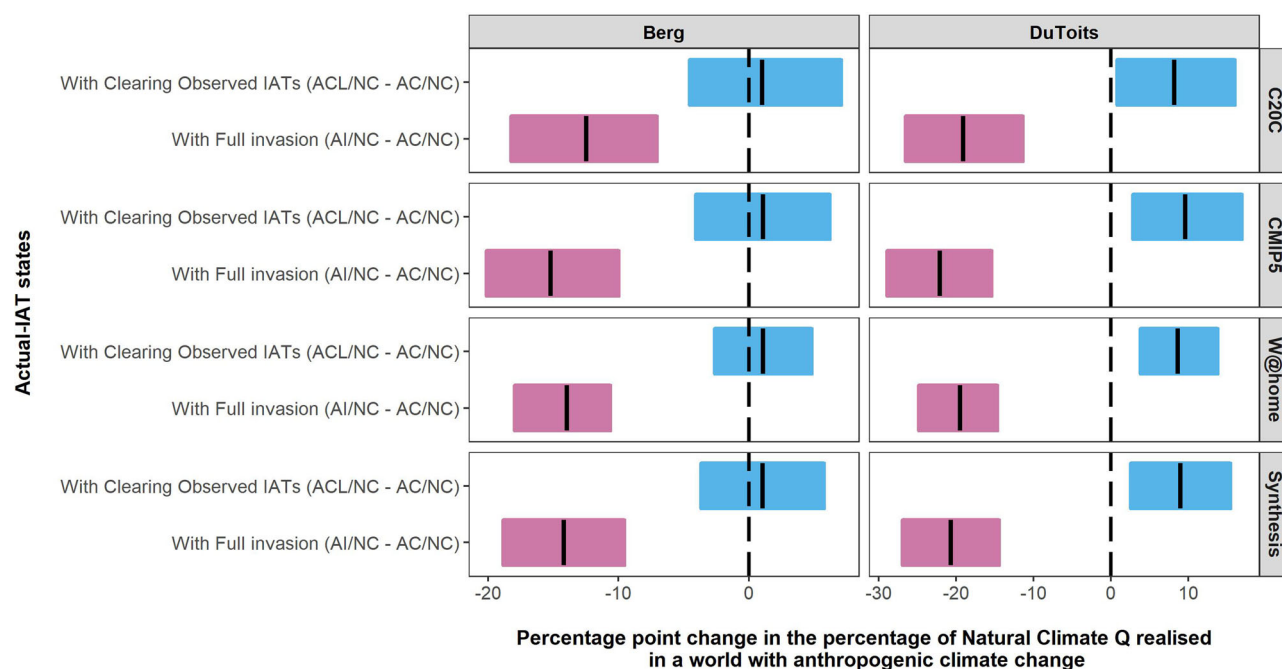


Fig. 5 The impact of IAT clearing (and lack thereof) on ameliorating or exacerbating the reduction in 2015–2017 drought-period streamflow from anthropogenic climate change. For each catchment (Berg and Du Toits, South Africa), and for fully cleared or fully invaded IAT states, the difference in QR % relative to that for current IAT conditions are shown (QR% point difference) (also see Supplementary Table 2). Changes are shown for each climate model experiment (C20C, CMIP5 and W@home) and for the multi-model experiment synthesis (Synthesis). The solid line is the median change, while the coloured bar shows the 95% confidence interval (Methods and Supplementary Methods 1). NC Natural Current, AC Actual Current, ACL Actual Cleared, AI Actual Invaded.

an attributable increase (Supplementary Notes 1, Supplementary Figs. 4–5 and Supplementary Table 4). Although we do not analyse actual evapotranspiration, it is likely that the impact of ACC on actual evapotranspiration would be lower, as reduced rainfall in the drought would limit water available for evapotranspiration⁵³. Furthermore, when we run the hydrological model with and without ACC impact on reference evapotranspiration (i.e., with Actual reference evapotranspiration versus with Natural reference evapotranspiration) (Supplementary Methods 3) we see that from our sampled simulations we cannot be confident that reference evapotranspiration makes a difference to the impact of ACC on drought-period streamflow (Supplementary Notes 2, Supplementary Fig. 6 and Supplementary Table 5): the difference between running the model with and without Actual reference evapotranspiration ranges between –5 and 3% and –7 and 3% points for the Upper Berg and Du Toits catchments, respectively. These findings align with previous work which shows it was primarily the lack of rainfall driving the 2015–2017 meteorological drought experienced in the region³¹.

Conclusions

We fill a gap in the current climate change adaptation and impacts attribution literature by providing (i) an assessment of the attributable impact of ACC on drought-period streamflow in headwater catchments during the 2015–2017 southwestern Cape drought, and (ii) quantitative evidence that NbS can be an important adaptation approach that can support drought impact reduction in a changing climate. We focus on a scale at which the impacts of climate change on extremes are felt and at which climate adaptation decisions are made². We show the importance of managing vegetation cover in headwater catchments in the Mediterranean climate of the southwestern Cape for reducing the hydrological impact of ACC via extreme meteorological drought events.

Despite our regional focus, the results are of relevance to water-limited environments across the globe that are experiencing woody encroachment due to IATs and/or woody indigenous vegetation, such as grassland and savanna ecosystems^{37,41,46,49–51}. This is because, despite global concerns and often substantial management efforts at local and regional scales, invasive plant species continue to proliferate^{43,54}. Furthermore, in contrast to common perceptions, there is a predominance of studies reporting reduced water yields following forest and woody cover expansion or afforestation in former shorter vegetation ecosystems as opposed to increased water yields⁴¹. Therefore, our results support existing cautionary warnings for those promoting extensive tree planting in ecoregions (shrubland, savanna and grassland systems) that are not naturally comprised of extensive forested landscapes⁵. This is especially pertinent as current climate models might be overestimating the removal of atmospheric carbon by forests⁵⁵. Furthermore, not managing IATs might compromise the efficacy of other climate change adaptation efforts to achieve water security^{44,45}. However, NbS are context specific and therefore while afforestation and trees outside forest areas can be detrimental to water supplies in certain places across the globe, it is important to factor in the full spectrum of socio-economic benefits and disbenefits while considering the scale and the context within which the NbS is situated.

In the context of this study, we show that high cover of IATs (such as the 40% currently occurring in one of our catchments or under hypothetical full invasion in both catchments) can exacerbate the impact of ACC on drought-period streamflow and resulting water shortages, such as those experienced during the Cape Town ‘Day Zero’ drought. Furthermore, clearing IATs and maintaining IATs at low levels of invasion can reduce the

attributable ACC impact as it propagates through the hydrological system. Thus, continuous maintenance and upscaling of clearing efforts in areas of high invasion is an important mechanism to adapt to changing hydro-climatic extremes due to ACC. Efforts directed at strategically important headwater catchments will likely yield higher dividends. Within these catchments, in terms of tackling the impact of ACC, our results suggest greater benefit from clearing heavily invaded catchments (such as the 40% occurring in the Du Toits, and greater) and maintenance at low invasion levels (such as maintaining the 9% occurring in the Upper Berg), compared to the eradication of IATs in catchments with lower invasion levels (such as completely clearing the 9% occurring in the Upper Berg). We do however acknowledge the issues that come with leaving residual IAT populations as these can be a source of seed for re-invasion. Furthermore, there are benefits to clearing IAT other than climate change adaptation.

Two physical climate factors drive hydrological drought, rainfall and reference evapotranspiration. We found a strong attributable ACC influence on rainfall and a weak influence on reference evapotranspiration for the drought period. Our results agree with previous work in the region confirming that reduced rainfall in the current world due to ACC was the dominant driver of the 2015–2017 meteorological drought³¹, but we extend this to show it was also the dominant driver of the reduced streamflow experienced in these catchments during the drought. Our results are also consistent with global and regional climate projections, all showing strong drying projections and that future increase in drought risk could be predominantly precipitation-driven for the Western Cape of South Africa^{31,56}. Our results however are in contrast to findings for the Okavango River system where a reduction in flood risk was attributed to higher temperatures (and thus evaporation) in the current world with little difference in rainfall simulated between a world with and without ACC²⁵.

NbS are important for reducing drought impact in our case study but did not completely offset the anthropogenic component of the drought we studied. As we expect meteorological drought risk to increase going forward due to further human influence on the climate^{31,32}, additional research should focus on understanding how the contribution of NbS to offsetting ACC could evolve in a world that is even warmer and drier or wetter than today. Further research is also needed to understand when and under what conditions human influence on the climate will eventually exceed the potential of NbS for reducing hydrological drought impact, while considering different NbS types and contexts across the globe^{57,58}. Furthermore, NbS must be fully integrated into a wider portfolio of water security adaptation options.

Methods

Catchments. The Du Toits and Upper Berg are upland fynbos-covered catchments feeding into the Berg and Breede Rivers in the southwestern Cape of South Africa (Table 2). The climate is Mediterranean and characterized by winter rainfall. Geology is typical of the mountains of the Cape Folded Belt of the Table Mountain Group and soils consist largely of sandstone-quartzitic soils which are highly leached and nutrient poor⁵⁹. Both catchments are extremely mountainous and form part of South Africa’s strategic water source areas providing high natural runoff and supporting the region’s population and economy. Strategic water source areas only cover 8% of South Africa but contribute substantially to development needs⁶⁰. The Upper Berg and Du Toits provide a critical source of water to the Western Cape Water Supply System, an integrated system of six large water impoundments which supply the City of Cape Town metropolis (58%), the agriculture sector (26%), smaller towns and nearby municipalities (6%), with ~10% lost to evaporation⁶¹. The Upper Berg catchment is the main source for the Berg Dam while the Du Toits is one of the main sources for the Theewaterskloof Dam. The Berg and Theewaterskloof Dams account for 15% and 53% of the Western Cape Water Supply System respectively⁶². The lack of rainfall experienced during 2015–2017 in both catchments manifested as hydrological drought with streamflow diminishing by 33% (Du Toits) and 45% (Upper Berg) of the long-term average.

Table 2 Catchment characteristics.

Catchment	Upper Berg	Du Toits	Source
Area (square kilometres)	78 km ²	46 km ²	Calculated for catchments derived from refs. ^{84,85}
Mean altitude (range) (masl)	761 (242–1591)	957 (358–1653)	ALOS DSM: Global 30 m ⁸⁵
Mean slope (degrees)	27	23	
Relief roughness (%): >160 = extremely dissected	279	246	^{86,87}
Mean annual rainfall (mm)	2553	1648	Estimated from various rainfall gauges and a distributed lapse rate ⁶³
Observed mean daily streamflow at gauges 2004–2017, 2015–2017 (% difference) (m ³ /s)	2.2, 1.2 (–45%)	1.2, 0.8 (–33%)	H6H007 Du Toits for catchment
Simulated daily streamflow at gauges 2004–2017, 2015–2017 (% difference) (m ³ /s)	2.2, 1.3 (–41%)	1.0, 0.7 (–30%)	G1H076 Berg for one tributary ⁸⁸
Simulated streamflow at catchment outlet 2004–2017, 2015–2017 (% difference) (m ³ /s)	4.2, 2.4 (–43%)	See above - gauge is at the outlet	Supplementary Table 6 and ⁶³
Observed reference evapotranspiration 2004–2017 (mm/day)	4.1		Observed: Penman Monteith reference evapotranspiration (local automatic weather station data ARC 30890)
Invasive alien tree infestation during drought years (%)	9	40	Derived at a 20 m × 20 m resolution from Sentinel 2 imagery ⁶⁷
Native Fynbos Shrubland high density during drought years (%)	36	23	
Native Fynbos Shrubland low density during drought years (%)	43	34	
Other land cover (bare, indigenous forest, wetland, urban, water, rock) (%)	12 (0.8; 0.6; 1.2; 0; 6.5; 2.8)	3 (0.2; 0.7; 0.2; 0.4; 0; 1.3)	

Characteristics of the two catchments in South Africa for which the climate-IAT states were modelled.

Both catchments had different levels of IAT invasion during the drought period (Fig. 2 and Table 2).

Hydrological model set-up and validation. The details of the model set up and evaluation are described in ref. ⁶³, so we only provide a summary here. We set up the MIKE SHE physically based hydrological model coupled with MIKE HYDRO River channel routing model to simulate the hydrological response of catchments to the four climate-IAT states at a daily time step. MIKE SHE has five process-oriented components of relevance to our two catchments: evapotranspiration (ET), overland and channel flow, unsaturated and saturated subsurface flow, and exchange between aquifers and rivers. Channel flow is represented by MIKE HYDRO River and thus a fully dynamic linkage between the river model and the other components is an integrated part of MIKE SHE.

We used a fully distributed implementation of MIKE SHE for both catchments to represent these major hydrological processes and their interactions. This entailed horizontally and vertically discretizing the catchments into an orthogonal network of three-dimensional grid squares (referred to as finite difference cells) to represent the spatial horizontal and vertical variability of catchment characteristics and input data. The model cell discretization was 60 m with a total of 32,400 and 48,400 cells for the Du Toits and Upper Berg respectively. The vertical depth of the saturated zone on average was 700 m and 900 m respectively for the Berg and Du Toits but this was distributed spatially based on existing estimated depth information on the Peninsula formation of the Table Mountain Aquifer Group for the region^{64–66}.

The overland flow zone was characterised based on land use and land cover data derived from Sentinel 2 imagery⁶⁷. Three main computational layers were used with variable thicknesses to describe vertical variations in the subsurface and their respective hydrogeological characteristics within each grid square. This included the unsaturated soil zone (1.5 m deep), the saturated zone, including a perched talus and weathered sandstone aquifer (15 m deep) to mimic subsurface piston flow typical of these catchments⁶⁸, and a spatially distributed deep Table Mountain Group Aquifer (average depths 700 and 900 m, respectively for the Berg and Du Toits).

Characteristics and parameterisations for the overland flow zone and subsurface layers were derived from various approaches including field sampling and laboratory analyses (unsaturated zone soil properties including soil depths, parameter values for the van Genuchten model for soil water retention⁶⁹, river channel cross sections, and leaf area indices) and literature review combined with calibration processes (saturated zone layers, depths, horizontal and vertical hydraulic properties, specific storage and yields). Algorithms used included the Kristensen and Jensen equations to calculate actual transpiration and soil evaporation based on several evapotranspiration parameters; diffusive wave approximation of the Saint Venant Equations based on the finite-difference formulation for overland flow; vertical flow in the soil zone was modelled using Richards' Equation, which solves for pressure head variation in the unsaturated zone; and groundwater flow in the saturated zone was modelled using the three-

dimensional Darcy Equation. We linked the overland flow and groundwater flow modules in MIKE SHE to a channel network by coupling with the MIKE Hydro River hydrodynamic river module. This coupling enabled one-dimensional simulation of river flows and water levels using the fully dynamic Saint Venant Equations.

Meteorological input data included daily rainfall and reference evapotranspiration data from local station data available for the catchments. This included eight local stations all of which provided rainfall data and one provided reference evapotranspiration data. The rainfall station data were interpolated across both model surfaces at the model resolution using an elevation-correction to account for orographic influence on rainfall.

Both Upper Berg and Du Toits catchment models performed satisfactorily relative to other studies of hydrological model performance⁷⁰, with <9% difference in daily mean streamflow compared to observations and including Nash-Sutcliffe efficiencies of above 0.58 (log transformed: 0.74), *r* values >0.77 and percent bias between –4 and –10 for daily data (Supplementary Fig. 7 and Supplementary Table 6; for the full description of the model set up and parameterisations see ref. ⁶³). Furthermore, the final models were shown to simulate the hydrological impacts of IATs accurately and in line with paired-catchment studies in the area⁶³.

Climate change attribution inputs to the hydrological model. We used 29 general circulation models (GCMs), comprising 27 Coupled atmosphere-ocean and 2 Atmospheric, altogether contributing 290 simulations of the southwestern Cape drought (1 January 2015 to 31 December 2017). Simulations represented two climate states: (i) Actual (145 simulations); and (ii) Natural (145 simulations) (Table 3).

Atmospheric general circulation models (AGCMs) are prescribed with sea surface temperatures (SSTs) to isolate the component of atmospheric variability driven by oceanic boundary forcing by eliminating the influence of the atmosphere on the ocean. They are useful for determining how the atmospheric circulation and land-surface climate might respond to a given set of surface boundary conditions^{71,72}. On the other hand, Coupled atmosphere-ocean general circulation models (CGCMs) allow a dynamically interacting ocean, although simulated SSTs do not necessarily track those observed⁷³.

Both the C20C and W@home experiments involve running many simulations of AGCMs differing only in their initial conditions and so representing possible trajectories of the climate system under a given set of time-evolving boundary conditions. We used simulations from ECHAM5.4 from the C20C experiment⁷⁴ as it was the only AGCM in C20C that fully covered the drought period. The Weather@home model from the Climate Prediction.net experiment is a 50 km Hadley Centre Regional Model (HadRM3P) for the southern African regional domain nested in the Hadley Centre Global Atmospheric Model (HadAM3P-N96)^{75,76}.

For the AGCMs, Actual simulations represented possible realisations of the drought (in this case daily precipitation and temperature data) under 2015–2017

Table 3 Climate model data underpinning the two climate states.

Model experiments	Model name/s	Models	Climate states (Actual and Natural)	Ensemble members per state	Total drought simulations
Atmospheric general circulation models (AGCMs)					
Climate Prediction.net distributed computing platform (referred to as W@home)	Weather@home	1	2	68	136
Climate of the 20th Century Plus (C20C+) Detection and Attribution project (referred to as C20C)	ECHAM5.4	1	2	50	100
Coupled general circulation models (CGCMs)					
Fifth phase of Coupled Model Intercomparison Project (referred to as CMIP5)	Supplementary Table 7	27	2	27	54
Totals		29		145	290

Model experiments and the number of models and ensemble members used in this study to represent the drought period (2015–2017).

observed boundary conditions. This included simulations forced by observed sea surface temperature (SST), sea ice concentration (SIC), GHG and aerosols. In contrast, Natural simulations represented possible realisations of the drought in the absence of anthropogenic interference with the climate system. This included naturalised (detrended and adjusted) SSTs and SICs without an ACC signal and pre-industrial GHG and aerosols (e.g., boundary conditions representing the 1880s)⁷⁴.

For the CMIP5 CGCMs, we used a combination of the historical runs and future runs from the first ensemble member (r1i1p1) of each of 27 models from the Coupled Model Intercomparison Project 5 (CMIP5) under a high emission scenario (representative concentration pathway 8.5, RCP8.5)^{77,78}. Unlike AGCMs, which are forced by observed SST, CGCMs are uncorrelated with real-world climate and therefore do not capture the drought period specifically over the years 2015–2017. Therefore, we extracted two periods of 31 years each, 1869–1899 and 2001–2031, representing the Natural and the Actual climate states respectively. For each of these 31-year periods, we then extracted the driest consecutive three years based on a 3-year running average to represent the most extreme drought periods across the models that could be considered analogues to the observed drought.

All climate models were evaluated specifically for the southwestern Cape analysis domain, at a scale that matches the GCM resolutions, using precipitation observations from the University of East Anglia Climate Research Unit (CRU) and reanalysis data from the European Centre for Medium-Range Weather Forecasts (ECMWF – ERA version 5: ERA5) (Supplementary Methods 4). We found that the models were able to reproduce seasonal and spatial variations of the observed rainfall to a satisfactory level (Supplementary Notes 3, Supplementary Figs. 8–9), and that bias correction (see below paragraph) addressed any major deficiencies affecting the inputs to the hydrological model (Supplementary Figs. 10–11).

We extracted daily precipitation, minimum temperature and maximum temperature from each climate model simulation from the corresponding nearest model grid point to each rainfall or reference evapotranspiration observed station used to drive the hydrological model. Data were extracted for a period of 15 years (2004–2018) for the AGCMs and 31 years (1869–1899 and 2001–2031) for the CGCMs for both the Actual and Natural climate states. We derived reference evapotranspiration from the temperature data using the Hargreaves and Samani approach⁷⁹. It is important to note that the resolution of the climate models (Supplementary Table 7) is far from resolving the resolution used in the hydrological modelling (i.e., 60 m by 60 m) and even in relation to the size of the full catchments. Therefore, before isolating the drought years for analysis from the climate data and running these in the hydrological models, we bias corrected the climate model data using a standard quantile-quantile bias correction approach^{80,81} based on the nearest observed station driving the baseline hydrological model. For the Actual climate state, quantile-quantile bias correction was performed by using a 20-day moving window around each day in all years to generate empirical cumulative distribution functions (ECDF) for the data for both observed station and climate model data. The quantiles for the observed station data were then mapped onto the corresponding model quantiles and the value for the observed data extracted as the new bias-corrected daily value. For the Natural climate state, we aligned the daily quantiles for each of the simulations with the corresponding daily quantiles in the climate model data from the Actual climate state, and then used the corresponding observed station quantile value as the bias-corrected value. Bias correction further improved the correlations with inter-annual and seasonal variations of local rainfall observation stations (Supplementary Figs. 10–11).

Attribution analysis. We quantified the impact of ACC on drought-period streamflow and the difference that IAT invasion or clearing could have had on this impact using two main metrics: (i) QR% (Table 4); and (ii) QR% point difference (Table 5).

QR% is the drought-period mean streamflow (Q) for each comparator state (Actual Current, -Cleared, -Invaded) expressed as a percentage of the reference state (Natural Current) drought-period streamflow (Table 4). For example, considering the first comparator (Actual Current) in relation to the reference state (as shown in Table 4) the equation is:

$$QR\% = (Q_i/Q_0) * 100 \tag{1}$$

where Q_i is the simulated mean daily streamflow for the Actual climate and Current IAT state (AC) during the drought period and Q_0 is the simulated mean daily streamflow for the Natural climate and Current IAT state (NC). For this metric a value <100% implies that drought-period streamflow would be lower than the reference and a value >100% implies that drought period streamflow would be higher. For reference and ease we also calculated the inverse of this and refer to it as the % Change in Q which is the percentage change in drought-period streamflow for each comparator Actual-IAT state in relation to the reference Natural Current state (Table 4, Supplementary Table 1).

QR% point difference (Table 5) is the difference between the QR% derived for the Actual Current in relation to the reference state (Actual Current/Natural Current [AC/NC]) (row 1 in Table 4) and the QR% derived for the other two comparator states (Actual Invaded, -Cleared) i.e., AI/NC and ACL/NC, respectively in row 2 and 3 in Table 4. A QR% point difference of zero indicates that there is no difference between the impact of ACC on drought-period streamflow with or without IAT clearing or invasion (Table 5). This is because the QR% for the Actual Current in relation to the Natural Current assesses the impact of ACC only as for both climate-IAT states we have the same IAT state, but the climate states are different. Therefore, differencing this value from the QR% derived for the other two comparator states shows the extent to which IAT invasion or clearing could have altered or offset this impact.

In place of significance levels (p values) and null hypotheses we used a bootstrap percentile confidence interval methodology^{47,48} to calculate a median and 95% confidence interval estimate for QR% (including % Change in Q) and QR% point difference. This entailed resampling the simulations of drought-period streamflow in each climate model experiment 1000 times for each pair of climate-IAT states (Supplementary Methods 1), which resulted in a bootstrapped sample of 1000 means of drought-period streamflow for each climate-IAT state (NC, AC, ACL, AI) and for each climate model experiment (W@home, C20C, and CMIP5). This bootstrapping approach was propagated through to the calculation of QR% (including % Change in Q) and QR% point difference⁸².

To summarise our results, for each climate model experiment and climate-IAT state we calculated the median and 95% percentiles for QR% and QR% point difference (2.5–97.5 percentiles, the latter of which we refer to as 95% Confidence Intervals [95%CI])⁸². The critical aspect is that relying on the bootstrap percentile methodology of generating 95% confidence intervals for our estimates and propagating this through the differencing allows us to provide an interval of plausible results with 95% confidence (i.e., we do not know the true result, but we can provide an interval of likely results with 95% confidence for this true result). For example, if the confidence interval generated for the differences includes the value zero, we cannot say with 95% confidence that IAT management in fact did have a detectable impact on the influence of ACC on drought-period streamflow (Table 5).

In addition to providing results for each climate model experiment, we also generated a synthesis of the results across climate model experiments using the mean of the medians for each climate model experiment, with equal weighting, along with 95% confidence intervals generated using the pooled standard deviation of the climate model experiments, following⁸³. We show the results rounded to zero decimal places in Results but provide these rounded to two decimal places in the Supplementary Information (Supplementary Tables 1–2). We also conducted the same attribution analysis and bootstrapping approach for the rainfall and reference evapotranspiration hydrological model driving input data (Supplementary Methods 2).

Table 4 Formulae used to calculate the drought-period streamflow (Q) ratio (QR), expressed as a percentage (QR%) and the % Change in Q for paired climate-invasive alien tree (climate-IAT) states.

No.	Climate-IAT state names	Code	QR%	% Change in Q	Reference	What effect are we assessing?	Inference based on bootstrapped confidence intervals of QR%
1	ActualCurrent/ NaturalCurrent	AC/ NC	$Q_i/Q_0 \times 100$	$(Q_i - Q_0)/Q_0 \times 100$	Natural Current: Natural Climate with observed levels of IATs that were present during the drought period	ACC only because the IAT state is the same as the reference IAT state.	100% = no impact of ACC on Q >100% = ACC increased Q <100% = ACC reduced Q
2	ActualInvaded/ NaturalCurrent	AI/ NC	$Q_{AI}/Q_0 \times 100$	$(Q_{AI} - Q_0)/Q_0 \times 100$		ACC and an increase to a fully invaded state from the reference IAT state.	100% = no impact of ACC + invasion >100% = ACC + invasion increased Q <100% = ACC + invasion reduced Q
3	ActualCleared/ NaturalCurrent	ACL/ NC	$Q_{ACL}/Q_0 \times 100$	$(Q_{ACL} - Q_0)/Q_0 \times 100$		ACC and a decrease to a completely cleared IAT state from the reference IAT state.	100% = no impact of ACC + clearing >100% = ACC + clearing increased Q <100% = ACC + clearing reduced Q

This table presents formulae used to isolate the impact of anthropogenic climate change (ACC) compared to the combined impact of ACC and (i) invasive alien tree (IAT) clearing; or (ii) lack thereof. For all calculations, the reference state is the Natural Current (i.e., Natural Climate and Current (observed) IAT levels that were present during the drought (column labelled Reference)). In all cases, we compared the Actual-IAT states to this same reference state (NC). We indicate the isolated impact that we are assessing in the column (What effect are we assessing?) and lastly provide a reminder of what this means in terms of the bootstrapped confidence interval methodology (last column).

Table 5 Formulae used to calculate the percentage point difference between the QR% for the paired climate-IAT states to show potential of invasive alien tree (IAT) management in modulating the impact of anthropogenic climate change on drought-period streamflow in South Africa.

Difference	QR% point difference	Explanation	Inference based on bootstrapped confidence intervals
AI/NC- AC/NC (2-1 in Table 4)	$(Q_{AI}/Q_0 \times 100) - (Q_i/Q_0 \times 100)$	The role of IAT management in modulating (exacerbating or ameliorating) reductions in drought-period streamflow due to ACC	0 = there is no difference between the impact of ACC on Q with or without invasion. <0 = allowing invasion exacerbated the reductions in Q due to ACC >0 = allowing invasion ameliorated the reductions in Q due to ACC
ACL/NC- AC/NC (3-1 in Table 4)	$(Q_{ACL}/Q_0 \times 100) - (Q_i/Q_0 \times 100)$		0 = there is no difference between the impact of ACC on Q with or without clearing. <0 = clearing exacerbated the reductions in Q due to ACC >0 = clearing ameliorated the reductions in Q due to ACC

The table presents formulae used to determine the extent to which IAT clearing or the lack thereof could have played a role in modulating the impact of anthropogenic climate change (ACC) on drought-period mean streamflow. We provide a reminder of what this means in terms of the bootstrapped confidence interval methodology (last column).

Data availability

The datasets generated in this study are available from ZivaHub, powered by Figshare for Institutions. This includes streamflow data in cumecs generated from running MIKE-SHE coupled with MIKE HYDRO River system to simulate the hydrological response of catchments to the four climate-Invasive Alien Tree (climate-IAT) states at a daily time step. The data, including meta data, can be accessed here: <https://doi.org/10.25375/uct.16684846>. This is the source data for Figs. 4, 5.

Code availability

Example code used to generate the QR%, % Change in Q and QR% point difference from the datasets shared above is available from ZivaHub, powered by Figshare for Institutions. The link is the same as the one above: <https://doi.org/10.25375/uct.16684846>.

Received: 20 September 2021; Accepted: 10 February 2022;

Published online: 09 March 2022

References

- IPCC. in *Climate Change 2021: The Physical Science Basis. Contribution of Working Group I to the Sixth Assessment Report of the Intergovernmental Panel on Climate Change* (eds Masson-Delmotte, V. et al) (Cambridge University Press. In Press, 2021).
- Otto, F. E. L. et al. Toward an inventory of the impacts of human-induced climate change. *Bull. Am. Meteorol. Soc.* **101**, E1972–E1979 (2020).

3. Stanners, D. et al. in *Sustainability Indicators. A Scientific Assessment* (eds Moldan, B., Hak, T. & Dahl, A. L.) 127–144 (Island Press, 2007).
4. Cohen-Shacham, E. et al. Core principles for successfully implementing and upscaling Nature-based Solutions. *Environ. Sci. Policy* **98**, 20–29 (2019).
5. Seddon, N. et al. Getting the message right on nature-based solutions to climate change. *Glob. Chang. Biol.* <https://doi.org/10.1111/gcb.15513> (2021).
6. Keesstra, S. et al. The superior effect of nature based solutions in land management for enhancing ecosystem services. *Sci. Total Environ.* **610–611**, 997–1009 (2018).
7. Seddon, N. et al. Understanding the value and limits of nature-based solutions to climate change and other global challenges. *Philos. Trans. R. Soc. Lond. B Biol. Sci.* **375**, 20190120 (2020).
8. Gómez Martín, E., Máñez Costa, M. & Schwerdtner Máñez, K. An operationalized classification of Nature Based Solutions for water-related hazards: from theory to practice. *Ecol. Econ.* **167** <https://doi.org/10.1016/j.ecolecon.2019.106460> (2020).
9. Doswald, N. et al. Effectiveness of ecosystem-based approaches for adaptation: review of the evidence-base. *Clim. Dev.* **6**, 185–201 (2014).
10. Chausson, A. et al. Mapping the effectiveness of nature-based solutions for climate change adaptation. *Glob. Chang. Biol.* <https://doi.org/10.1111/gcb.15310> (2020).
11. Rebelo, A. J., Holden, P. B., Esler, K. & New, M. G. Benefits of water-related ecological infrastructure investments to support sustainable land-use: a review of evidence from critically water-stressed catchments in South Africa. *R. Soc. Open Sci.* **8**, 201402 (2021).
12. Berrang-Ford, L. et al. A systematic global stocktake of evidence on human adaptation to climate change. *Nat. Clim. Change* **11**, 989–1000 (2021).
13. Griscom, B. W. et al. Natural climate solutions. *Proc. Natl Acad. Sci. USA* **114**, 11645–11650 (2017).
14. Bastin, J.-F. et al. The global tree restoration potential. *Science* **365**, 76–79 (2019).
15. Koch, A., Brierley, C. & Lewis, S. L. Effects of Earth system feedbacks on the potential mitigation of large-scale tropical forest restoration. *Biogeosciences* **18**, 2627–2647 (2021).
16. Girardin, C. A. J. et al. Nature-based solutions can help cool the planet - if we act now. *Nature* **593**, 191–194 (2021).
17. Sudmeier-Rieux, K. et al. Scientific evidence for ecosystem-based disaster risk reduction. *Nat. Sustain.* **4**, 803–810 (2021).
18. Otto, F. E. L. Attribution of weather and climate events. *Annu. Rev. Environ. Resources* **42**, 627–646 (2017).
19. Philip, S. et al. A protocol for probabilistic extreme event attribution analyses. *Adv. Stat. Climatol. Meteorol. Oceanogr.* **6**, 177–203 (2020).
20. Herring, S. C., Christidis, N., Hoell, A., Hoerling, M. P. & Stott, P. A. Explaining extreme events of 2019 from a climate perspective. *Bull. Amer. Meteorol. Soc.* **102**, S1–S112 (2021).
21. Otto, F. E. L. et al. Challenges to understanding extreme weather changes in lower income countries. *Bull. Am. Meteorol. Soc.* <https://doi.org/10.1175/bams-d-19-0317.1> (2020).
22. Pall, P. et al. Anthropogenic greenhouse gas contribution to flood risk in England and Wales in autumn 2000. *Nature* **470**, 382–385 (2011).
23. Kay, A. L., Crooks, S. M., Pall, P. & Stone, D. A. Attribution of Autumn/Winter 2000 flood risk in England to anthropogenic climate change: a catchment-based study. *J. Hydrol.* **406**, 97–112 (2011).
24. Schaller, N. et al. Human influence on climate in the 2014 southern England winter floods and their impacts. *Nat. Clim. Change* **6**, 627–634 (2016).
25. Wolski, P., Stone, D., Tadross, M., Wehner, M. & Hewitson, B. Attribution of floods in the Okavango basin, Southern Africa. *J. Hydrol.* **511**, 350–358 (2014).
26. Ross, A. C. et al. Anthropogenic influences on extreme annual streamflow into Chesapeake Bay from the Susquehanna River. *Bull. Am. Meteorol. Soc.* **102**, S25–S32 (2021).
27. Mitchell, D. et al. Attributing human mortality during extreme heat waves to anthropogenic climate change. *Environ. Res. Lett.* **11**, 074006 (2016).
28. Botai, C., Botai, J., de Wit, J., Nongwane, K. & Adeola, A. Drought Characteristics over the Western Cape Province, South Africa. *Water* <https://doi.org/10.3390/w9110876> (2017).
29. Wolski, P. How severe is Cape Town's "Day Zero" drought? *Significance* **15**, 24–27 (2018).
30. Stafford, L., Shemie, D., Kroeger, T., Baker, T. & Apse, C. *The Greater Cape Town Water Fund. Assessing the return on investment for Ecological Infrastructure restoration. Business case.* (The Nature Conservancy, 2018).
31. Otto, F. E. L. et al. Anthropogenic influence on the drivers of the Western Cape drought 2015–2017. *Environ. Res. Lett.* <https://doi.org/10.1088/1748-9326/aae9f9> (2018).
32. Pascale, S., Kapnick, S. B., Delworth, T. L. & Cooke, W. F. Increasing risk of another Cape Town "Day Zero" drought in the 21st century. *Proc. Natl. Acad. Sci. USA* <https://doi.org/10.1073/pnas.2009144117> (2020).
33. Van Wilgen, B. W., Measey, J., Richardson, D. M., Wilson, J. R. & Zengeya, T. A. *Biological Invasions in South Africa* (Springer Nature, 2020).
34. Le Maitre, D. et al. Impacts of plant invasions on terrestrial water flows in South Africa in *Biological Invasions in South Africa* (eds van Wilgen, B. W., Measey, J., Richardson, D. M., Wilson, J. R. & Zengeya, T. A.) 431–457 (Springer, 2020).
35. Brown, A. E., Zhang, L., McMahon, T. A., Western, A. W. & Vertessy, R. A. A review of paired catchment studies for determining changes in water yield resulting from alterations in vegetation. *J. Hydrol.* **310**, 28–61 (2005).
36. Dennedy-Frank, P. J. & Gorelick, S. M. Insights from watershed simulations around the world: watershed service-based restoration does not significantly enhance streamflow. *Glob. Environ. Change* <https://doi.org/10.1016/j.gloenvcha.2019.101938> (2019).
37. Calder, I. D. & Dye, P. Hydrological impacts of invasive alien plants. *Land Use Water Resour. Res.* **7**, 1–12 (2001).
38. Trabucco, A., Zomer, R. J., Bossio, D. A., van Straaten, O. & Verchot, L. V. Climate change mitigation through afforestation/reforestation: a global analysis of hydrologic impacts with four case studies. *Agric. Ecosyst. Environ.* **126**, 81–97 (2008).
39. Farley, K. A., Jobbagy, E. G. & Jackson, R. B. Effects of afforestation on water yield: a global synthesis with implications for policy. *Glob. Change Biol.* **11**, 1565–1576 (2005).
40. Jackson, R. B. Trading water for carbon with biological carbon sequestration. *Science* **310**, 1944–1947 (2005).
41. Filoso, S., Bezerra, M. O., Weiss, K. C. B. & Palmer, M. A. Impacts of forest restoration on water yield: a systematic review. *PLoS ONE* **12**, e0183210 (2017).
42. Sitzia, T., Campagnaro, T., Kowarik, I. & Trentanovi, G. Using forest management to control invasive alien species: helping implement the new European regulation on invasive alien species. *Biol. Invasions* **18**, 1–7 (2015).
43. Richardson, D. M. & Rejmánek, M. Trees and shrubs as invasive alien species - a global review. *Divers. Distrib.* **17**, 788–809 (2011).
44. Everard, M. et al. Can control of invasive vegetation improve water and rural livelihood security in Nepal? *Ecosyst. Serv.* **32**, 125–133 (2018).
45. Everard, M. Can management of 'thirsty' alien trees improve water security in semi-arid India? *Sci. Total Environ.* **704**, 135451 (2020).
46. Archer, S. R. et al. Woody plant encroachment: causes and consequences in *Rangeland Systems Springer Series on Environmental Management* (ed. Briske, D. D.) Chapter 2, 25–84 (2017).
47. Wood, M. Bootstrapped confidence intervals as an approach to statistical inference. *Organ. Res. Methods* **8**, 454–470 (2016).
48. Tan, S. H. The correct interpretation of confidence intervals. *Proc. Singapore Healthc.* **19** (2010).
49. Coetsee, C., Gray, E. F., Wakeling, J., Wigley, B. J. & Bond, W. J. Low gains in ecosystem carbon with woody plant encroachment in a South African savanna. *J. Trop. Ecol.* **29**, 49–60 (2012).
50. Stevens, N., Erasmus, B. F., Archibald, S. & Bond, W. J. Woody encroachment over 70 years in South African savannas: overgrazing, global change or extinction aftershock? *Philos. Trans. R. Soc. Lond. B Biol. Sci.* <https://doi.org/10.1098/rstb.2015.0437> (2016).
51. Venter, Z. S., Cramer, M. D. & Hawkins, H. J. Drivers of woody plant encroachment over Africa. *Nat. Commun.* **9**, 2272 (2018).
52. Forsyth, G. G., Le Maitre, D. C., Smith, J. & Lotter, D. *Upper Berg River Catchment (G10A) Management Unit Control Plan.* (Natural Resources Management (NRM) Department of Environmental Affairs, 2016).
53. Dirmeyer, P. A., Balsamo, G., Blyth, E. M., Morrison, R. & Cooper, H. M. Land-atmosphere interactions exacerbated the drought and heatwave over northern Europe during summer 2018. *AGU Adv.* **2**, e2020AV000283 (2021).
54. Rejmánek, M., Richardson, D. M. & Pysek, P. Trees and shrubs as invasive alien species - 2013 update of the global database. *Divers. Distrib.* **19**, 1093–1094 (2013).
55. Terrer, C. et al. A trade-off between plant and soil carbon storage under elevated CO₂. *Nature* **591**, 599–603 (2021).
56. Ziervogel, G. et al. Climate change impacts and adaptation in South Africa. *Wiley Interdiscip. Rev. Clim. Change* **5**, 605–620 (2014).
57. Thomas, A. et al. Global evidence of constraints and limits to human adaptation. *Reg. Environ. Change* <https://doi.org/10.1007/s10113-021-01808-9> (2021).
58. Dow, K., Berkhouf, F. & Preston, B. L. Limits to adaptation to climate change: a risk approach. *Curr. Opin. Environ. Sustain.* **5**, 384–391 (2013).
59. Manning, J. & Goldblatt, P. *Plants of the greater Cape Floristic Region 1: the Core Cape Flora.*, (South African National Biodiversity Institute, 2012).
60. Nel, J. L. et al. Strategic water source areas for urban water security: Making the connection between protecting ecosystems and benefiting from their services. *Ecosyst. Serv.* **28**, 251–259 (2017).
61. Wolski, P. What Cape Town learned from its drought. *Bull. At. Sci.* <https://thebulletin.org/2018/04/what-cape-town-learned-from-its-drought/> (2018).
62. D. W. S. Cape Town River Systems State of Dams on 2021-08-16. *Department of Water and Sanitation. Republic of South Africa.* <https://www.dws.gov.za/Hydrology/Weekly/RiverSystems.aspx?river=CT> (2021).

63. Rebelo, A. J. et al. The hydrological benefits of restoration: a modelling study of alien tree clearing in four mountain catchments in South Africa. Preprint at *J. Hydrol.* <https://doi.org/10.21203/rs.3.rs-1316834/v1>.
64. DWAF. *The Assessment of Water Availability in the Berg Catchment (WMA 19) by Means of Water Resource Related Models: Report 9 (Groundwater Model): Volume 9 (Breede River Alluvium Aquifer Model)*. (Department of Water Affairs and Forestry, 2008).
65. DWAF. *The Assessment of Water Availability in the Berg Catchment (WMA 19) by Means of Water Resource Related Models: Report 9 (Groundwater Model): Volume 3 (Regional Conceptual Model)*. (Department of Water Affairs and Forestry, 2008).
66. Blake, D., Mlisa, A. & Hartnady, C. Large scale quantification of aquifer storage and volumes from the Peninsula and Skurweberg Formations in the southwestern Cape. *Water SA* **36**, 177–184 (2010).
67. Holden, P. B., Rebelo, A. J. & New, M. G. Mapping invasive alien trees in water towers: a combined approach using satellite data fusion, drone technology and expert engagement. *Remote Sens. Appl.: Soc. Environ.* <https://doi.org/10.1016/j.rsase.2020.100448> (2021).
68. Midgley, J. & Scott, D. The use of stable isotopes of water in hydrological studies in the Jonkershoek Valley. *Water SA* **20**, 151–154 (1994).
69. Van Genuchten, M. T. A closed-form equation for predicting the hydraulic conductivity of unsaturated soils. *Soil Sci. Soc. Am. J.* **44**, 892–898 (1980).
70. Moriasi, D. N., Gitau, M. W., Pai, N. & Daggupati, P. Hydrologic and water quality models: performance measures and evaluation criteria. *Trans. ASABE* **58**, 1763–1785 (2015).
71. Stone, D. A. et al. A basis set for exploration of sensitivity to prescribed ocean conditions for estimating human contributions to extreme weather in CAM5.1-1degree. *Weather Clim. Extremes* **19**, 10–19 (2018).
72. Risser, M. D., Stone, D. A., Paciorek, C. J., Wehner, M. F. & Angéilil, O. Quantifying the effect of interannual ocean variability on the attribution of extreme climate events to human influence. *Clim. Dyn.* **49**, 3051–3073 (2017).
73. Jones, G. S., Stott, P. A. & Christidis, N. Attribution of observed historical near-surface temperature variations to anthropogenic and natural causes using CMIP5 simulations. *J. Geophys. Res. Atmos.* **118**, 4001–4024 (2013).
74. Sun, L. et al. Drivers of 2016 record Arctic warmth assessed using climate simulations subjected to factual and counterfactual forcing. *Weather Clim. Extremes* **19**, 1–9 (2018).
75. Guillod, B. P. et al. weather@home 2: validation of an improved global-regional climate modelling system. *Geosci. Model Dev.* **10**, 1849–1872 (2017).
76. Massey, N. et al. weather@home—development and validation of a very large ensemble modelling system for probabilistic event attribution. *Q. J. R. Meteorol. Soc.* **141**, 1528–1545 (2014).
77. Taylor, K. E., Stouffer, R. J. & Meehl, G. A. An overview of CMIP5 and the experiment design. *Bull. Am. Meteorol. Soc.* **93**, 485–498 (2012).
78. Flato, G. et al. in *Climate change 2013: the physical science basis. Contribution of Working Group I to the Fifth Assessment Report of the Intergovernmental Panel on Climate Change* 741–866 (Cambridge University Press, 2014).
79. Hargreaves, G. H. & Samani, Z. A. Reference crop evapotranspiration from temperature. *Appl. Eng. Agriculture* **1**, 96–99 (1985).
80. Cayan, D. R., Maurer, E. P., Dettinger, M. D., Tyree, M. & Hayhoe, K. Climate change scenarios for the California region. *Clim. Change* **87**, 21–42 (2008).
81. Cannon, A. J., Sobie, S. R. & Murdock, T. Q. Bias correction of GCM precipitation by quantile mapping: how well do methods preserve changes in quantiles and extremes? *J. Clim.* **28**, 6938–6959 (2015).
82. R Core Team. *R: A language and environment for statistical computing*. (R Foundation for Statistical Computing. <https://www.R-project.org/>, 2020).
83. Paciorek, C. J., Stone, D. A. & Wehner, M. F. Quantifying statistical uncertainty in the attribution of human influence on severe weather. *Weather Clim. Extremes* **20**, 69–80 (2018).
84. Tadono, T. et al. Generation of the 30 M-Mesh Global Digital Surface Model by Alos Prism. *ISPRS - International Archives of the Photogrammetry, Remote Sensing and Spatial Information Sciences* **XLI-B4**, 157–162, https://developers.google.com/earth-engine/datasets/catalog/JAXA_ALOS_AW3D30_V3_2#description (2016).
85. Takaku, J., Tadono, T., Tsutsui, K. & Ichikawa, M. Validation of "Aw3d" Global Dsm Generated from Alos Prism. *ISPRS Ann. Photogramm.* **III-4**, 25–31 (2016).
86. Viviroli, D. Increasing dependence of lowland population on mountain water resources. *Nat. Sustain.* **3**, 917–928 (2020).
87. Meybeck, M. A New typology for mountains and other relief classes: an application to global continental water resources and population distribution. *Mt. Res. Dev.* **21**, 34–45 (2001).
88. DWS. Surface water home. Department of Water and Sanitation. Republic of South Africa. <https://www.dws.gov.za/Hydrology/Unverified/UnverifiedDataFlowInfo.aspx> (2021).

Acknowledgements

We are grateful for funding for this research from the AXA Research Fund, through the AXA Research Chair in African Climate Risk, the Danish Ministry of Foreign Affairs (MFA) [grant number 17-M07-KU], and the BNP Paribas Foundation Climate Initiative. We acknowledge the Agricultural Research Council, South African Weather Service, South African Environment Observation Network, Umvoto, the City of Cape Town, Zutari and the Cape Winelands Biosphere Reserve for data or assistance with data collection; EkoSource for assistance with hydrological model troubleshooting; and F Otto and N Fučkar at the University of Oxford for assistance with Weather@home data access. We would also like to thank the volunteers running the Weather@home models as well as the technical team in Oxford e-Research Centre (OeRC) for their support. We also acknowledge the World Climate Research Programme's Working Group on Coupled Modelling, which is responsible for CMIP, and we thank the climate modelling groups (listed in Supplementary Table 7) for producing and making available their model output. The C20C data were accessed using the science gateway resources of the National Energy Research Scientific Computing Center, a DOE Office of Science User Facility supported by the Office of Science of the U.S. Department of Energy under Contract No. DE-AC02-05CH11231.

Author contributions

M.G.N. conceived the research problem. P.B.H., P.W. and M.G.N. developed the joint-attribution framework. P.H. and A.R. set up the hydrological models. P.B.H., R.C.O., K.A.L., J.K. and T.N. generated the climate model data inputs. P.B.H. analysed the data. P.W. and M.G.N. provided supervisory support for all aspects of the research. P.B.H. wrote the manuscript with support from M.G.N. All authors contributed comments during the writing of the manuscript.

Competing interests

The authors declare no competing interests.

Additional information

Supplementary information The online version contains supplementary material available at <https://doi.org/10.1038/s43247-022-00379-9>.

Correspondence and requests for materials should be addressed to Petra B. Holden.

Peer review information *Communications Earth & Environment* thanks Daithi Stone, Mysiak Jaroslav and the other, anonymous, reviewer(s) for their contribution to the peer review of this work. Primary Handling Editors: Rahim Barzegar, Heike Langenberg. Peer reviewer reports are available.

Reprints and permission information is available at <http://www.nature.com/reprints>

Publisher's note Springer Nature remains neutral with regard to jurisdictional claims in published maps and institutional affiliations.



Open Access This article is licensed under a Creative Commons Attribution 4.0 International License, which permits use, sharing, adaptation, distribution and reproduction in any medium or format, as long as you give appropriate credit to the original author(s) and the source, provide a link to the Creative Commons license, and indicate if changes were made. The images or other third party material in this article are included in the article's Creative Commons license, unless indicated otherwise in a credit line to the material. If material is not included in the article's Creative Commons license and your intended use is not permitted by statutory regulation or exceeds the permitted use, you will need to obtain permission directly from the copyright holder. To view a copy of this license, visit <http://creativecommons.org/licenses/by/4.0/>.

© The Author(s) 2022